



**Repositorio Institucional de la Universidad Autónoma de Madrid**

<https://repositorio.uam.es>

Esta es la **versión de autor** del artículo publicado en:

This is an **author produced version** of a paper published in:

Angewandte Chemie - International Edition 54.8 (2015): 2543-2547

**DOI:** <http://dx.doi.org/10.1002/anie.201411272>

**Copyright:** © 2015 Wiley-VCH Verlag

El acceso a la versión del editor puede requerir la suscripción del recurso  
Access to the published version may require subscription

# Non-centrosymmetric Homochiral Supramolecular Polymers of Tetrahedral Subphthalocyanine Molecules

Julia Guilleme,<sup>[a]</sup> María J. Mayoral,<sup>[a]</sup> Joaquín Calbo,<sup>[b]</sup> Juan Aragón,<sup>[b]</sup> Pedro M. Viruela,<sup>[b]</sup> Enrique Ortí,<sup>[b]\*</sup> Tomás Torres<sup>[a],[c]\*</sup> and David González-Rodríguez<sup>[a]\*</sup>

**Abstract:** A combination of spectroscopy, microscopy, and computational studies reveal the formation of non-centrosymmetric homochiral columnar subphthalocyanine assemblies via a cooperative supramolecular polymerization process driven by hydrogen-bonding between amide groups,  $\pi$ - $\pi$  stacking, and dipolar interactions between axial dipolar B-F bonds.

Because of their singular structure, the columnar stacking of tetrahedral-shaped molecules can provide materials with exclusive properties that are not fulfilled by common planar  $\pi$ -conjugated discotics.<sup>1</sup> First, these molecules may exhibit intrinsic chirality,<sup>2</sup> which potentially leads to non-centrosymmetric stacks in which helical chirality evolves from the molecule itself,<sup>3</sup> and not from chiral centers present in side tails.<sup>4</sup> Second, they are often endowed with axial dipoles that may add up along the stacks resulting in polar nanostructures, which may be exploited for the electric-field uniaxial alignment of the columns<sup>5</sup> or for the development of polarized semiconducting films.<sup>6</sup> However, the supramolecular convex-concave polymerization of related bowl- or cone-shaped monomers represents in itself a challenging task.<sup>7</sup> Due to their 3D structure, most of them are obviously reluctant to aggregate in solution. Moreover, many bowl-shaped aromatics like corannulane, sumanene, calixarene, or cyclotrimeratrylene undergo cone inversion,<sup>8</sup> which leads to depolarization and stack racemization.

Subphthalocyanines (SubPcs; Figure 1a)<sup>9</sup> are one of those rare examples of  $\pi$ -conjugated aromatic molecules with rigid tetrahedral structure.<sup>10</sup> They are constituted by three isoindole units condensed around a boron atom, which also bears an axial ligand perpendicular to the macrocyclic core. Contrasting with their higher analogues, the phthalocyanines (Pcs), whose supramolecular chemistry is dominated by  $\pi$ - $\pi$  interactions between planar surfaces, SubPcs do not exhibit a strong tendency to aggregate in solution. Such quality, certainly stemming from their non-planar geometry, has proven beneficial for many applied fields in which dye aggregation needs to be prevented.<sup>11</sup> However, due to their intense absorption and emission in the visible and their tunable electronic properties,<sup>12</sup>

SubPcs have recently arisen a great deal of technological interest in the fields of organic semiconductors and optoelectronics.<sup>13</sup> Such applications often demand suitable columnar organizations in which close  $\pi$ - $\pi$  contacts contribute to efficient exciton and charge transport.<sup>1</sup>

Here, we show for the first time that tetrahedral-shaped molecules like SubPcs can be polymerized in solution into self-assembled non-centrosymmetric homochiral columnar nanostructures. The key to overcome the challenging head-to-tail (convex-concave) stacking is the combination of hydrogen-bonding interactions between three peripheral amide groups and the use of an axial fluorine atom, which provides a minimal steric hindrance upon stacking<sup>7c</sup> and a strong axial dipole moment.

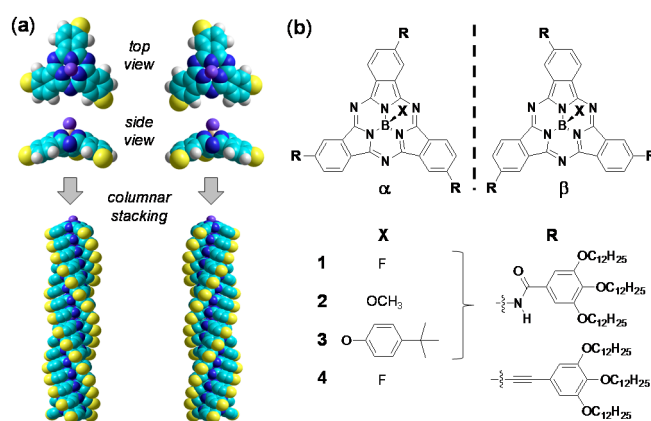


**Figure 1.** (a) Top and side views of the two enantiomers of a model trisubstituted SubPcBF macrocycle and the corresponding homochiral head-to-tail columnar stacks. (b) Structure of the two enantiomers of compound **1** (**1 $\alpha$**  and **1 $\beta$** ),<sup>14,15</sup> and compounds **2**, **3** and **4**.

$C_3$ -symmetric SubPcs **1**, **2**, **3**, and **4** (Figure 1b) were synthesized as racemic mixtures and characterized as described in the Supporting Information. The two enantiomers of **1**, hereafter called **1 $\alpha$**  and **1 $\beta$** , were then separated by analytical chiral HPLC (see Figure S1) in the milligram scale.<sup>15</sup>

First insights into the aggregation of enantiomers **1 $\alpha$**  or **1 $\beta$**  in solution came from absorption and emission spectroscopy. In 1,4-dioxane, a competing solvent for hydrogen-bonding, compounds **1 $\alpha/\beta$**  display the characteristic narrow Q-band features of monomeric SubPcs, that is, a maximum at 576 nm ( $\epsilon = 86.000 \text{ M}^{-1} \text{ cm}^{-1}$ ) with shoulders at 530 and 560 nm. In sharp contrast, **1 $\alpha/\beta$**  solutions in methylcyclohexane (MCH) or dodecane exhibit a broader, blue-shifted Q-band with maximum at 520 nm ( $\epsilon = 38.000 \text{ M}^{-1} \text{ cm}^{-1}$ ) (Figures 2a,b and S2).<sup>16</sup> Likewise, **1 $\alpha/\beta$**  in dioxane show the typical SubPc strong emission band with a maximum at 590 nm, whereas MCH solutions are virtually non-emissive (Figures 2c,d and S2). Both the presence of the small axial fluorine atom and the peripheral amide substituents

[a] J. Guilleme, Dr. M. J. Mayoral, Dr. D. González-Rodríguez, Prof. T. Torres

Departamento de Química Orgánica, Facultad de Ciencias, Universidad Autónoma de Madrid, 28049 Madrid, Spain  
E-mail: david.gonzalez.rodriguez@uam.es, tomas.torres@uam.es

[b] J. Calbo, Dr. J. Aragón, Dr. P. M. Viruela, Prof. E. Ortí  
Instituto de Ciencia Molecular, Universidad de Valencia, 46980 Paterna (Valencia), Spain  
E-mail: enrique.orti@uv.es

[c] Prof. T. Torres  
IMDEA Nanociencia, Facultad de Ciencias  
Cantoblanco, 28049 Madrid, Spain

Supporting information for this article is given via a link at the end of the document.

are required for these spectroscopic changes in apolar solvents, since none of compounds **2**, **3**, and **4** display such features. Hence, we attribute the spectral fingerprints found in apolar solvents to head-to-tail columnar supramolecular polymers of **1 $\alpha$ / $\beta$** , as depicted in Figure 1a. CD spectroscopy was consistent with this hypothesis (Figures 2e,f). Compounds **1 $\alpha$**  or **1 $\beta$**  in the monomer state exhibit a mirror-imaged CD signal centered at 578 nm, negative for **1 $\alpha$**  and positive for **1 $\beta$** .<sup>14</sup> In MCH, in contrast, *M*- and *P*-helical homochiral stacks are formed that show a Cotton effect with a zero-crossing at the 520 nm aggregate absorption maximum. Hydrogen-bonding between the exocyclic amide groups was confirmed by <sup>1</sup>H NMR and FT-IR.

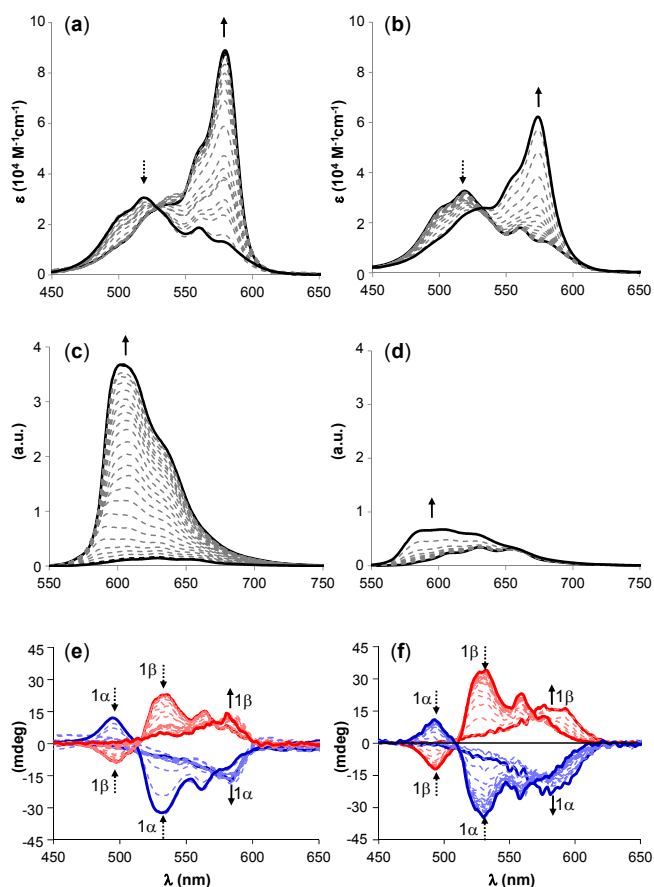


**Figure 2.** SubPc **1 $\beta$**  Q-band absorption (a,b), emission (c,d) and CD (e,f) changes as a function of: (a,c,e) the volume fraction of dioxane ( $\chi_d$ ) in MCH:dioxane mixtures (from  $\chi_d = 0$  to 0.35; [**1 $\beta$** ] =  $5.0 \times 10^{-5}$  M), or (b,d,f) the temperature ( $T$ ) (from 368 to 268 K; [**1 $\beta$** ] =  $3.9 \times 10^{-6}$  M) in MCH solutions. Arrows indicate the trends with increasing  $\chi_d$  or  $T$ , respectively.

The dissociation of **1 $\alpha$ / $\beta$**  stacks can be followed by spectroscopy with changes in sample concentration, temperature, or solvent composition. Figures 2a, 2c, and 2e show respectively the absorption, emission, and CD changes occurring in the transition from the supramolecular polymer to the monomer as the volume fraction of dioxane ( $\chi_d$ ) in MCH:dioxane mixtures is increased. Increasing the sample temperature of MCH solutions results in similar changes (Figures 2b, 2d, and 2f). Consistent with a supramolecular polymerization process, the degree of aggregation ( $\alpha$ ) decreases at high temperatures and at low

concentrations (Figure S3). The self-assembly mechanism has been analyzed by fitting the non-sigmoidal cooling curves, calculated from the UV/vis absorption coefficient at 576 nm, to the cooperative nucleation–elongation model developed by Meijer and co-workers (Figure S4).<sup>17</sup> This model assumes that upon an unfavourable nucleation process, the system can abruptly elongate yielding extended supramolecular polymeric species. The data fitted reasonably well to a dimeric nucleus that then grows by successive SubPc stacking.<sup>18</sup> Applying the model to **1 $\alpha$ / $\beta$**  in MCH, we obtained the main thermodynamic parameters, both for the nucleation:  $\Delta H^\circ_{\text{nuc}} = -11.7 \pm 1.3$  kJ mol<sup>-1</sup> and  $K_{\text{nuc}} = 7.1 \times 10^3$  M<sup>-1</sup>, as well as for the elongation process:  $\Delta H^\circ_e = -56.1 \pm 3.4$  kJ mol<sup>-1</sup>,  $\Delta S^\circ = -55.0 \pm 2.8$  J mol<sup>-1</sup> K,  $K_e = 4.2 \times 10^5$  M<sup>-1</sup>, and  $T_e = 344.9 \pm 1.1$  K. The degree of cooperativity in the self-assembly process was calculated at  $\sigma = 0.017$ .<sup>15,16</sup> These values agree reasonably well with those reported for other hydrogen-bonded polymers obtained from C<sub>3</sub>-symmetric monomers. Our entropic term is, however, relatively small, which may reflect the high structural rigidity of our SubPc monomers.<sup>18b</sup>

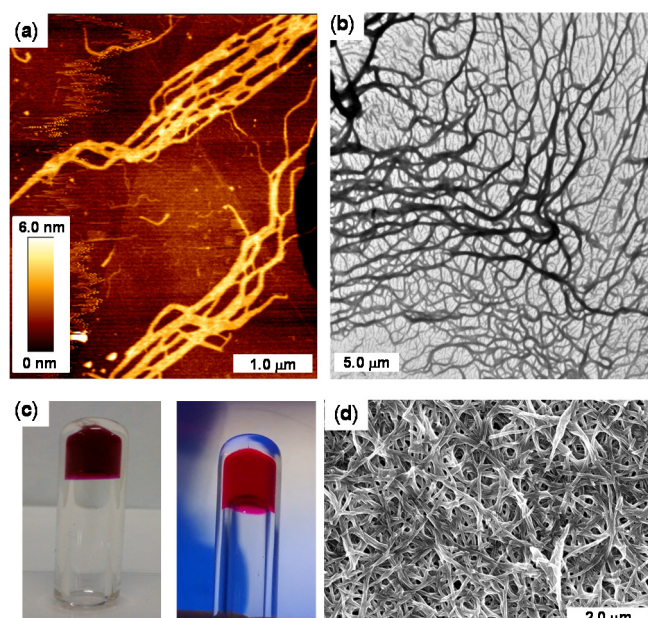


**Figure 3.** (a) AFM height image of drop-casted **1** ([**1**] =  $3.2 \times 10^{-6}$  M in MCH) onto HOPG. (b) TEM image of a negatively stained **1** MCH solution on a carbon-coated copper grid. (c) Dodecane gels under no (left) or 365 nm (right) UV irradiation. (d) SEM image of the corresponding xerogel.

The formation of supramolecular polymeric stacks of SubPcs **1 $\alpha$ / $\beta$**  was confirmed by scanning probe and electron microscopies. MCH solutions were dropcasted onto highly-oriented pyrolytic graphite (HOPG) and the surface was imaged by AFM after solvent evaporation. As shown in Figure 3a, long fibrillar objects were observed on the surface whose heights match those of single SubPc fibers (2.5 nm in diameter) and fiber bundles (5–6 nm), likely formed by bundling of 2 or 3 individual fibers. The high propensity of these fibers to bundle may be the reason why we could not observe helical structures. TEM analysis (Figure 3b) also showed the formation of bundled fibers in MCH or dodecane. In addition, SubPc **1** formed stable red-magenta gels in dodecane at a concentration of 4.2 mg/mL, whose

fluorescence emission is quenched with respect to non-aggregated solutions in dioxane (Figure 3c). SEM images of the xerogel (Figure 3d), prepared by vacuum-drying the dodecane gels, revealed an extended and interconnected fibrous network.

Intrigued by these unique non-centrosymmetric homochiral assemblies, quantum-chemical calculations were carried out to gain further insight into the structural features of the head-to-tail stacks of  $1\alpha/\beta$  at the molecular scale. We took  $1\beta$  as the model enantiomer, but the analysis performed hereafter can be equally applied to  $1\alpha$ . Prior to optimizing a columnar structure, we examined the diverse conformational possibilities for the H-bonding association between amides. In  $1\alpha/\beta$  there are 4 types of amide conformations, depending on the C-C-N-H dihedral angle formed between this group and the isoindole ring (Figure 4a). *Syn-in* and *anti-out* conformations are complementary and lead to left-handed (*M*) helices, whereas *syn-out* and *anti-in* conformations result in right-handed (*P*) helices (Figure S5). To discriminate which conformation is energetically favored, we considered three different issues: intermolecular interactions, net dipole moment, and chiral helicity.

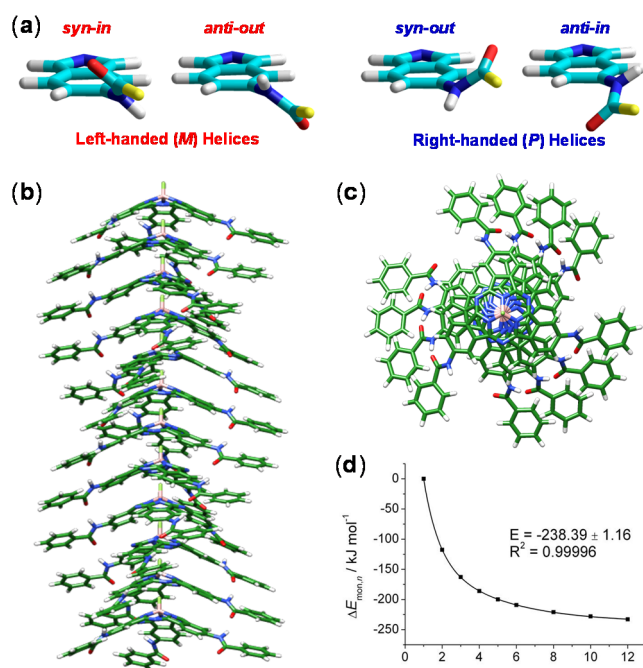


**Figure 4.** (a) Amide conformations that lead to triple intermolecular H-bonding in the  $1\beta$  helical stacks. We can define *syn* and *anti* orientations – depending whether the amide carbonyl dipole is aligned parallel or antiparallel, respectively, to the axial B–F bond –, and *in* and *out* orientations – as a function of the position of the carbonyl oxygen with respect to the isoindole ring –. (b,c) Side and top views of *P*-helical *all-anti-in* head-to-tail arrangement of  $1\beta$  stacks calculated by DFT. (d) Stabilization energy per monomer unit ( $\Delta E_{\text{mon},n}$ ) calculated at the at  $\omega$ B97X-D/cc-pVTZ level as the number of monomers ( $n$ ) in the *all-anti-in* aggregate increases. Energy values are fitted to a biexponential decay function (solid line).

First, head-to-tail  $1\beta$  dimers were built and fully optimized at the B97-D/6-31G\*\* level (Figures S6–S8). Right-handed *syn-out* and *anti-in* conformations lead to *P*-helical dimers stabilized by both  $\pi$ - $\pi$  and H-bonding interactions between the three amide

groups (see Figure S8). A significantly different situation is however noted for *M*-helical *syn-in* and *anti-out* conformations, for which theoretical models reveal that the amide groups cannot adopt an optimal orientation for H-bond formation and the dimers are, as a result, considerably destabilized.<sup>15</sup> Further comparison between *syn-out* and *anti-in* dimers (Figure S9) showed that, although both dimers present similar structural parameters, the *anti-in* arrangement is computed 7.8 kcal/mol more stable than the *syn-out* associate.

In order to explain this energy difference we then considered discrete interactions between dipoles. As the stack grows, a global dipole is generated along the *z* axis that feeds from two main contributions: i) the axial B–F bond, which leads to a rigid dipole that increases with stack length,<sup>6b</sup> and ii) the *z*-component of the amide carbonyl dipole, which can change orientation in order to add (*syn*) or subtract (*anti*) to the B–F dipole.<sup>5</sup> A vacuum environment, where theoretical calculations were carried out, or solvents with low dielectric constants like MCH or dodecane, are not suited to stabilize polar structures. Hence, we reasoned that the non-centrosymmetric stacks of  $1\alpha/\beta$  must grow with a minimum global dipole moment, which may be achieved by participation of *anti* conformations. Calculations show that columnar aggregates having the three amides in the *anti-in* conformation, *i.e.*, their *z*-component dipoles opposing the B–F dipole, have minimum net dipole moments (Figure S12).

Finally, the theoretical CD spectrum was computed for both the monomer and trimer species of  $1\beta$  (Figure S10). For the monomer, only one positive CD signal is predicted, in agreement with the experimental results (Figure S1). However, a more intense, blue-shifted, negative-to-positive CD signal is predicted for the *anti-in* right-handed trimer of  $1\beta$  (Figure S10a), which also reproduces the experimental CD spectra (Figures 2e,f) and confirms the *P*-helicity of the columnar stacks formed by  $1\beta$ . The theoretical CD spectrum computed for the less stable *P*-helical *syn-out* conformation of  $1\beta$  (Figure S10b) significantly differs from the experimental data, so this conformation was again ruled out.<sup>15</sup> A similar analysis was made for  $1\alpha$  that corroborates the formation of *all-anti-in M*-helical stacks.

In summary, theoretical calculations select the *anti-in* as the most stable configuration for the triple array of H-bonds in our homochiral SubPc assemblies. This amide conformation maximizes intermolecular interactions, leads to a minimum net dipole moment in the stacking direction, and reproduces the experimental CD spectra of the assemblies.<sup>19</sup> With this information in hand,  $1\beta$  *all-anti-in* columnar aggregates of increasing size – up to the dodecamer – were built up and theoretically investigated by using the long-range corrected  $\omega$ B97X-D functional and the more extended triple- $\zeta$  cc-pVTZ basis set.<sup>20</sup> As observed in Figure 4b,c, a right-handed *anti-in* helical stacking favors the coexistence of intermolecular H-bonding,  $\pi$ - $\pi$  stacking, and dipolar interactions. Neighboring molecules are separated by 4.12 Å and rotated by 23.0°. This torsional angle, which establishes that 16 molecules are necessary to complete one helical pitch, is dictated by the triple array of H-bonds. The amide groups are twisted out the plane of the isoindole units by 36.5° to maximize the intermolecular H-bonding interactions, and give rise to NH $\cdots$ O intermolecular

contacts of 1.93 Å. Intermolecular C...C contacts between the isoindole phenyl rings of neighbouring molecules in the 3.50–4.10 Å range are found, indicating that, despite the steric effect of the axial ligand, stabilizing  $\pi$ - $\pi$  interactions are also present in these columnar arrangements. The  $F^{\delta-}\cdots B^{\delta+}$  contacts between adjacent molecules are calculated at 2.78 Å, which are just slightly longer than two times the covalent B–F bond (1.37 Å) and significantly shorter than the sum of the van der Waals radii of boron (1.92 Å) and fluorine (1.47 Å). This evidences strong dipolar interaction between B–F dipoles along the stacks, which may account for their remarkable stability as noted before in the spectroscopic studies.

Figure 4d shows the stabilization energy per monomer unit ( $\Delta E_{\text{mon},n}$ ) calculated for (**1 $\beta$** )<sub>n</sub> all-anti-in columnar aggregates with increasing number of monomeric units ( $n = 1$ –6, 8, 10, 12). As the columnar stack grows, the H-bonding network strengthens due to the larger polarization, and the aggregate becomes more stable. It is worth noting that the asymptotic limit ( $n = \infty$ ) is rapidly approached upon addition of 10–12 monomer units, being the increase in stabilization relatively small from then on. The stabilization per monomer unit predicted for the dodecamer is –232.9 kJ/mol, very close to that obtained from the extrapolation to  $n = \infty$  (–238.4 kJ/mol). The enhancement in  $\Delta E_{\text{mon},n}$  with  $n$  suggests a large cooperative character for the self-association of SubPc **1**, in agreement with the experiments.

We have demonstrated for the first time the formation of non-centrosymmetric homochiral columnar SubPc assemblies via a cooperative supramolecular polymerization process driven by a combination of non-covalent interactions: H-bonding,  $\pi$ - $\pi$  stacking, and dipolar interactions between axial dipolar B–F bonds. Future work will focus on profiting from the axial dipole moments generated in these assemblies to produce electric-field responsive polar materials that may exhibit ferroelectricity.

## Acknowledgements

Funding from MINECO (CTQ2011-24187, CTQ2011-23659, MAT2012-38538-CO3-01 and 02, CTQ2012-31914, and CTQ2012-35513-CO2-01), CAM (S2013/MIT-2841 FOTO-CARBON), GVA (PROMETEO/2012/053), and MECD (F.P.U. fellowship (J. G.)) is gratefully acknowledged.

**Keywords:** Subphthalocyanine • Supramolecular Polymerization • Porphyrinoids • Self-assembly • Homochiral Aggregates

- [1] S. Laschat, A. Baro, N. Steinke, F. Giesselmann, C. Hägele, G. Scalia, R. Judele, E. Kapatsina, S. Sauer, A. Schreivogel, M. Tosoni, *Angew. Chem. Int. Ed.* **2007**, *46*, 4832–4887; *Angew. Chem.* **2007**, *119*, 4916–4973.
- [2] a) S. Shimizu, A. Miura, S. Khene, T. Nyokong, N. Kobayashi, N. *J. Am. Chem. Soc.* **2011**, *133*, 17322–17328; b) G. Markopoulos, L. Henneicke, J. Shen, Y. Okamoto, P. G. Jones, H. Hopf, *Angew. Chem. Int. Ed.* **2012**, *51*, 12884–12887; *Angew. Chem.* **2012**, *124*, 13057–1306.
- [3] K. Sato, Y. Itoh, T. Aida, *Chem. Sci.* **2014**, *5*, 136–140.
- [4] A. R. A. Palmans, E. W. Meijer, *Angew. Chem. Int. Ed.* **2007**, *46*, 8948–8969; *Angew. Chem.* **2007**, *119*, 9106–9126.
- [5] a) D. Miyajima, F. Araoka, H. Takezoe, J. Kim, K. Kato, M. Takata, T. Aida, *Angew. Chem. Int. Ed.* **2011**, *50*, 7865–7869; *Angew. Chem.* **2011**, *123*, 8011–8015; b) D. Miyajima, F. Araoka, H. Takezoe, J. Kim, K. Kato, M. Takata, T. Aida, *Science*, **2012**, *336*, 209–213.
- [6] T. Amaya, S. Seki, T. Moriuchi, K. Nakamoto, T. Nakata, H. Sakane, A. Saeki, S. Tagawa, T. Hirao, *J. Am. Chem. Soc.* **2009**, *131*, 408–409.
- [7] The head-to-tail columnar stacking of cone- or bowl-shaped molecules has been, however, demonstrated in crystal and liquid crystal structures. See: a) M. Sawamura, K. Kawai, Y. Matsuo, K. Kanie, T. Kato, E. Nakamura, *Nature* **2002**, *419*, 702–705; b) H. Sakurai, T. Daiko, H. Sakane, T. Amaya, T. Hirao, *J. Am. Chem. Soc.* **2005**, *127*, 11580–11581; c) S. Rodríguez-Morgade, C. G. Claessens, A. Medina, D. González-Rodríguez, E. Gutierrez-Puebla, A. Monge, I. Alkorta, J. Elguero, T. Torres, *Chem. Eur. J.* **2008**, *14*, 1342–1350; d) A. S. Filatov, E. A. Jackson, L. T. Scott, M. A. Petrukhina, *Angew. Chem. Int. Ed.* **2009**, *48*, 8473–8476; *Angew. Chem.* **2009**, *121*, 8625–8628; e) D. Miyajima, K. Tashiro, F. Araoka, H. Takezoe, J. Kim, K. Kato, M. Takata, T. Aida, *J. Am. Chem. Soc.* **2009**, *131*, 44–45.; f) B. M. Schmidt, S. Seki, B. Topolinski, K. Ohkubo, S. Fukuzumi, H. Sakurai, D. Lentz, *Angew. Chem. Int. Ed.* **2012**, *51*, 11385–11388; g) J. G. Brandenburg, S. Grimme, P. G. Jones, G. Markopoulos, G. Hopf, M. K. Cyranski, D. Kuck, *Chem. Eur. J.* **2013**, *19*, 9930–9338.
- [8] a) Y.-T. Wu, J. S. Siegel, *Chem. Rev.* **2006**, *106*, 4843–4867; b) T. Amaya, T. Hirao, *Chem. Commun.* **2011**, *47*, 10524–10535.
- [9] a) C. G. Claessens, D. González-Rodríguez, T. Torres, *Chem. Rev.* **2002**, *102*, 835–853; b) S. Shimizu, N. Kobayashi, *Chem. Commun.* **2014**, *50*, 6949–6966; c) C. G. Claessens, D. González-Rodríguez, M. S. Rodríguez-Morgade, A. Medina, T. Torres, *Chem. Rev.* **2014**, *114*, 2192–2277.
- [10] S. Samdal, H. V. Volden, V. R. Ferro, J. M. García de la Vega, D. González-Rodríguez, T. Torres, *J. Phys. Chem. A* **2007**, *111*, 4542–4550.
- [11] a) C. G. Claessens, D. González-Rodríguez, T. Torres, G. Martín, F. Agulló-López, I. Ledoux, J. Zyss, V. R. Ferro, J. M. García de la Vega, *J. Phys. Chem.* **2005**, *109*, 3800–3806; b) H. Xu, X.-J. Jiang, E. Y. M. Chan, W.-P. Fong, D. K. P. Ng, *Org. Biomol. Chem.* **2007**, *5*, 3987–3992; c) D. González-Rodríguez, E. Carbonell, D. M. Guldi, T. Torres, *Angew. Chem. Int. Ed.* **2009**, *48*, 8032–8036; *Angew. Chem.* **2009**, *121*, 8176–8180; d) D. González-Rodríguez, E. Carbonell, G. de Miguel Rojas, C. Atienza Castellanos, D. M. Guldi, T. Torres, *J. Am. Chem. Soc.* **2010**, *132*, 16488–16500.
- [12] a) D. González-Rodríguez, T. Torres, D. M. Guldi, J. Rivera, M. A. Herranz, L. Echegoyen, *J. Am. Chem. Soc.* **2004**, *126*, 6301–6313; b) D. González-Rodríguez, C. G. Claessens, T. Torres, S.-G. Liu, L. Echegoyen, N. Vila, S. Nonell, *Chem. Eur. J.* **2005**, *11*, 3881–3893.
- [13] a) X. Tong, S. R. Forrest, *Org. Electron.* **2011**, *12*, 1822–1825; b) G. E. Morse, J. S. Castrucci, M. G. Helander, Z.-H. Lu, T. P. Bender, *ACS Appl. Mater. Interfaces* **2011**, *3*, 3538–3544; c) S. M. Menke, W. A. Luhman, R. J. Holmes, *Nature Mater.* **2012**, *12*, 152–157.
- [14] The structure of enantiomers **1 $\alpha$**  and **1 $\beta$**  was assigned on the basis of their CD signature compared to literature data for related SubPcs (ref. 2a), as well as on their DFT-computed theoretical CD spectra.
- [15] See the Supporting Information for further details.
- [16] Data for **1 $\beta$** . Racemic **1** or pure enantiomers **1 $\alpha$**  or **1 $\beta$**  display similar spectroscopic features in the different solvents studied.
- [17] a) A. J. Maarkvort, H. M. M. ten Eikelder, P. A. J. Hilbers, T. F. A. de Greef, E. W. Meijer, *Nat. Commun.* **2011**, *2*, 509; b) H. M. M. ten Eikelder, A. J. Markvoort, T. F. A. de Greef, P. A. J. J. Hilbers, *J. Phys. Chem. B*, **2012**, *116*, 5291–5301.
- [18] a) M. J. Mayoral, C. Rest, V. Stepanenko, J. Schellheimer, R. Q. Albuquerque, G. Fernández, *J. Am. Chem. Soc.* **2013**, *135*, 2148–2151; b) F. García, P. A. Korevaar, A. Verlee, E. W. Meijer, A. R. A. Palmans, L. Sánchez, *Chem. Commun.* **2013**, *49*, 8674–8676; c) C. Rest, M. J. Mayoral, K. Fucke, J. Schellheimer, V. Stepanenko, G. Fernández, *Angew. Chem. Int. Ed.* **2014**, *53*, 700–705; *Angew. Chem.* **2014**, *126*, 716–722.

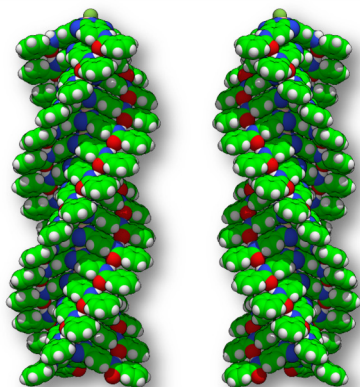
- [19] N. Kobayashi, A. Muranaka, J. Mack, *Circular Dichroism and Magnetic Circular Dichroism Spectroscopy for Organic Chemists*, RSC Publishing, Cambridge, **2012**.
- [20] The monomer used to build up the oligomers and the relative disposition of the adjacent molecules along the stack were obtained from the  $\omega$ B97X-D/6-31G\*\* fully optimized structure of the heptamer (see the Supporting information for full computational details).
-

## Entry for the Table of Contents

### COMMUNICATION

---

**Piling up** rigid tetrahedral-shaped subphthalocyanine dye molecules in a convex-to-concave fashion results in unconventional homochiral non-centrosymmetric columnar assemblies.



*Julia Guilleme, María J. Mayoral, Joaquín Calbo, Juan Aragón, Pedro M. Viruela, Enrique Ortí,\* David González-Rodríguez,\* and Tomás Torres\**

**Page No. – Page No.**

**Non-centrosymmetric Homochiral Supramolecular Polymers of Tetrahedral Subphthalocyanine Molecules**

---